Relevance of Human Aldoketoreductases and Microbial β-Glucuronidases in Testosterone Disposition

Abdul Basit[1], John K. Amory[2], Vijaya Saradhi Mettu[1], Cindy Yanfei Li[3], Scott Heyward[4], Parth B. Jariwala[5], Matthew R. Redinbo[5] and Bhagwat Prasad[1]

[1]Department of Pharmaceutical Sciences, Washington State University, Spokane, WA

[2]Department of Medicine, University of Washington, Seattle, WA

[3]Department of Pharmaceutics, University of Washington, Seattle, WA

[4]BioIVT Inc., Baltimore, MD

[5]Departments of Chemistry, Biochemistry and Microbiology, and the Integrated Program for Biological and Genome Sciences, University of North Carolina at Chapel Hill, Chapel Hill, NC, USA.

Running title: AKRs and GUSs in Testosterone Disposition

The total number of manuscript pages: 34

The total number of figures: 5

The total number of tables: 0

Total word count of the Abstract: 243

Total word count of the Introduction: 801

Total word count of the Discussion: 779

Corresponding author: Bhagwat Prasad, Ph.D., Department of Pharmaceutical Sciences,

Washington State University, Spokane, WA 99202, USA. Phone: +1-509-358-7739. Fax: +1

509-368-6561. Email: bhagwat.prasad@wsu.edu

ABBREVIATIONS:

3α, 5β -THT: 3α, 5β -Tetrahydrotestosterone

5ß-DHT: 5β-Dihydrotestosterone

AG: Androsterone glucuronide

AGC: Automatic gain control

AKR: Aldoketoreductase

ALDH: Aldehyde dehydrogenase

CNV: Copy number variation

DDA: Data-dependent acquisition

DHCR: Dehydrocholesterol reductase

DHTG: Dihydrotestosterone glucuronide

EtioG: Etiocholanolone glucuronide

GAHT: Gender-affirming hormone therapy

GUS: β-Glucuronidase

HSD: Hydroxysteroid dehydrogenase

MRP: Multi-drug resistance associated proteins

OATP: Organic anion transporting polypeptide

OPLS-DA: Orthogonal partial least squares discriminant analysis

PCA: Principal component analysis

TG: Testosterone glucuronide

TRT: Testosterone replacement therapy

UGT: Uridine 5'-diphospho-glucuronosyltransferase

ABSTRACT

Testosterone exhibits high variability in pharmacokinetics and glucuronidation after oral administration. While testosterone metabolism has been studied for decades, the impact of UGT2B17 gene deletion and the role of gut bacterial β-glucuronidases on its disposition are not well characterized. We first performed an exploratory study to investigate the effect of UGT2B17 gene deletion on the global liver proteome, which revealed significant increases in proteins from multiple biological pathways. The most upregulated liver proteins were aldoketoreductases (AKR1D1, AKR1C4, AKR7A3, AKR1A1, 7-dehydrocholesterol reductase (DHCR7)) and alcohol or aldehyde dehydrogenases (ADH6, ADH1C, ALDH1A1, ALDH9A1, and ALDH5A). In vitro assays revealed that AKR1D1 and AKR1C4 inactivate testosterone to 5β-dihydrotestosterone (5β-DHT) and 3α, 5β-tetrahydrotestosterone (3α, 5β-THT), respectively. These metabolites also appeared in human hepatocytes treated with testosterone and in human serum collected after oral testosterone dosing in men. Second, we evaluated the fate of testosterone glucuronide (TG) secreted into the intestinal lumen and its potential reactivation into testosterone. Incubation of TG with purified gut microbial β-glucuronidase (GUS) enzymes and with human fecal extracts confirmed testosterone reactivation by gut bacterial enzymes. Our exploratory study suggests that testosterone is metabolized by AKRs to 5β-DHT and 3α, 5β-THT in individuals harboring a UGT2B17 deletion, and these metabolites are then eliminated through glucuronidation by another UGT isoforms, UGT2B7. Both testosterone metabolic switching and variable testosterone activation by gut microbial enzymes are important mechanisms for explaining disposition of orally administered testosterone, and appear essential to unraveling the molecular mechanisms underlying UGT2B17-associated pathophysiological conditions.

SIGNIFICANCE STATEMENT

We investigated the association of UGT2B17 gene deletion and the role of gut bacterial β-glucuronidases on testosterone disposition in vitro. The experiment revealed upregulation of AKR1D1 and AKR1C4 and their role to inactivate testosterone to 5β-dihydrotestosterone and 3α, 5β-tetrahydrotestosterone, respectively. Key gut bacterial species responsible for testosterone glucuronide activation were identified. These data are important for explaining disposition of exogenously administered testosterone and appear essential to unraveling the molecular mechanisms underlying UGT2B17-associated pathophysiological conditions.

INTRODUCTION

Testosterone is an essential hormone that is important for male reproduction and the maintenance of secondary sexual characteristics, bone mineral density, and muscle mass. Testosterone masculinizing gender-affirming hormone therapy (GAHT) and testosterone replacement therapy (TRT) are the front-line treatment options for transgender and hypogonadal men, respectively (Schlich and Romanelli, 2016; Spanos et al., 2020). Although >23 million Americans are seeking testosterone therapy, high interindividual variability in testosterone disposition is associated with high risk-to-benefit ratios (Bhasin et al., 2006; Bhasin et al., 2010; Bhasin and Matsumoto, 2010; Swerdloff et al., 2015; Spanos et al., 2020). Variable testosterone pharmacokinetics (PK) can result unpredictable side effects including severe cardiovascular side effects (Bhasin et al., 2006; Bhasin et al., 2010; Bhasin and Matsumoto, 2010; FDA, 2015; Schlich and Romanelli, 2016), which have led to a "black-box" warning issued regarding the testosterone label by the U.S. Food and Drug Administration (FDA). Further, as urinary testosterone is used as a biomarker of testosterone doping, variable testosterone disposition is associated with inaccurate anti-doping testing (Jakobsson et al., 2006; Schulze et al., 2008; Schulze et al., 2009; Strahm et al., 2015). Thus, variability in testosterone disposition presents critical challenges for the safe and effective GAHT and TRT as well as for accurate anti-doping testing and enforcement.

Exogenously administered testosterone through oral, intramuscular, or topical routes shows significant interindividual variability in its PK irrespective of the route of administration (Mazer et al., 2005; Wilson et al., 2018). The variable testosterone PK is likely due to the first-pass metabolism and poor bioavailability, involvement of polymorphic transport and elimination, release from the depot site, and/or prodrug activation (Rane and Ekstrom, 2012). Regarding testosterone metabolism, 17β-hydroxysteroid dehydrogenases (17β-HSDs), 5α-reductases, and UDP-glucuronosyltransferase 2B17 (UGT2B17) play important roles in converting testosterone

to its primary metabolites, androstenedione, dihydrotestosterone (DHT), and TG, respectively (Fig. 1) (Basit et al., 2018). We have shown that testosterone and its secondary but major inactive unconjugated metabolites (androsterone and etiocholanolone) extensively primarily metabolized by glucuronidation (Basit et al., 2018), where the average serum concentration time (AUC) profiles of TG, androsterone glucuronide (AG), and etiocholanolone glucuronide (EtioG) are 80, 380, and 85-fold higher than the unconjugated testosterone after 800 mg oral testosterone dosing.

UGT2B17 is a highly variable human testosterone metabolizing enzyme. Copy number variation (CNV) and single nucleotide polymorphisms (SNPs) as well as non-genetic factors (age and sex) are associated with variable UGT2B17 expression and activity (Bhatt and Prasad, 2018; Zhang et al., 2018). Interestingly, the distribution of UGT2B17 CNV shows a high population variation, with deletion frequencies ranging from ~15% in Nigerians to >90% in Japanese population (Xue et al., 2008). UGT2B17 deletion is linked to diseases such as prostate cancer (Kpoghomou et al., 2013; Gauthier-Landry et al., 2015), osteoporosis, and obesity (Zhu et al., 2015). The urinary excretion of testosterone as a glucuronide is reduced by 90%, a significant change, in UGT2B17 deletion subjects compared to UGT2B17 high expressers (Jakobsson et al., 2006; Juul et al., 2009). However, the serum testosterone concentration in the deletion group is only 15% higher when compared to UGT2B17 expressers (Yang et al., 2008). We hypothesize that this discrepancy is likely due to the presence of other, potentially compensatory metabolic pathways in the UGT2B17 deletion group.

We have also shown that TG formed in the liver and intestine can be eliminated into bile, intestinal lumen or blood through multi-drug resistance associated proteins, MRP2 and MRP3 (Li et al., 2019). Our recent findings also suggest that organic anion transporting polypeptide (OATP1B) transporters can uptake TG into the liver, which is then available for efflux into the bile (Li et al., 2020). These data suggest that TG elimination to bile and intestine is more

favored over its transport into the blood. Because glucuronide metabolites are generally activated by bacterial β-glucuronidase (GUS) enzymes present in commensal microbiota (Ervin et al., 2019), we hypothesized that the high concentrations of serum androgen glucuronides are likely deconjugated to their respective unconjugated forms. While AG and EtioG represent inactivation pathways in testosterone metabolism, TG and dihydrotestosterone glucuronide (DHTG) could be reactivated to testosterone and DHT through the actions of bacterial GUS proteins. Consistent with our hypothesis, a recent study showed that high concentrations of free DHT are found in the colonic contents of specific pathogen free mice but are not observed in germ-free mice (Collden et al., 2019). Thus, it is important to investigate the interplay between various mechanisms of testosterone inactivation and reactivation catalyzed by both host gut microbial gene products.

The first aim of this study was to investigate the association of UGT2B17 gene deletion with the liver proteome. The hypothesis generating proteomics data revealed upregulation of unique androgen metabolic pathways, which were then evaluated through a series of *in vitro* and *in vivo* data. Second, we characterized the potential gut microbial GUS enzymes that can activate TG into testosterone.

MATERIALS AND METHODS

Materials

Steroid and steroid conjugate standards were purchased either from Cerilliant Corp (Round Rock, TX) or Steraloid (Newport, RI). LC-MS/MS grade acetonitrile, methanol, acetone, and formic acid were procured from Fisher scientific (Fair Lawn, NJ). Recombinant human UGT2B7, UGT2B15 and UGT2B17 Supersomes™ were purchased from Corning Inc. (Corning, NY). Trypsin, iodoacetamide (IAA), dithiothreitol (DTT), and bovine serum albumin were purchased from Thermo Fisher Scientific (Rockford, IL). Ammonium bicarbonate (ABC) with 98% purity

was purchased from Acros Organics (Geel, Belgium), whereas alamethicin, cofactor UDP-glucuronic acid (UDPGA), magnesium chloride, and di– and mono-basic potassium phosphate were purchased from Sigma-Aldrich (St. Louis, MO). Custom synthesized surrogate peptides for targeted proteomics analysis were procured from Thermo Fisher Scientific (Rockford, IL). Cryopreserved primary human hepatocytes (n = 4) as well as hepatocyte thawing (HT) and hepatocyte incubation (HI) media were kindly provided by BioIVT Inc. (Baltimore, MD). Liver S9 fraction and cytosol samples were procured from liver tissues from the Human Liver Bank of University of Washington School of Pharmacy (Seattle, WA) from our previous study (Bhatt and Prasad, 2018).

Untargeted proteomics analysis of liver S9 fraction

Sample preparation and LC-MS/MS acquisition: S9 fraction was isolated from previously genotyped UGT2B17 deletion (n=3; 2 males and 1 female) and high expressing (n=3; all males) liver samples for untargeted proteomics assay (Bhatt and Prasad, 2018). The total protein concentration was determined with bicinchoninic acid (BCA) assay and 80 µL (2 mg/mL) S9 fraction was transferred for trypsin digestion using a previously optimized method (Balhara et al., 2021). Briefly, the sample was mixed with 10 µL bovine serum albumin (BSA, 0.2 mg/mL) and reduced using 10 µL DTT (250 mM) at 95 °C for 10 min. After cooling the sample for 10 min, the denatured protein was subjected to alkylation using IAA (500 mM, 20 µL) in the dark at room temperature. The protein sample was precipitated with 1 mL ice-cold acetone followed by centrifugation at 16000 x g and 4 °C for 10 min. The pellet was collected and dried at room temperature (10 min) and washed with 0.5 mL ice cold methanol. After centrifugation at 8000 x g, the protein pellet was collected and dried for 30 min at room temperature and re-dissolved in 50 mM ammonium (60 µL) bicarbonate for trypsin digestion using 20 µL of trypsin solution (trypsin to protein ratio 1:100) at 37 °C for 16 hrs. The reaction was quenched with 5 µL 5% formic acid and centrifuged at 8000 x g (4°C for 5 min).

Tryptic peptides from the liver S9 fraction were analyzed in data-dependent acquisition (DDA) mode using Q-Exactive HF MS coupled with EASY-nLC 1200 system (Thermo Fisher Scientific, Waltham, MA). The tryptic digest (0.9 µg equivalent) was loaded onto Thermo Scientific™ Acclaim™ PepMap™ 100 C18 HPLC column with a mobile phase (0.1% formic acid in water (A) and 0.1% formic acid in acetonitrile (B)) at a flow rate of 0.3 µL/min. The following LC gradient program was used: 5% B (0-5 min), 5-25% B (5-105 min), 25-40% B (105-125 min), 40-95% B (125-126 min), and 95% B (126-136 min). The column temperature was 40 °C.

MS data were acquired using the DDA approach using top 10 ions (m/z range, 375–1500) from the survey scans. The full MS scanning was performed with automatic gain control (AGC) target set to $3e^6$ and a higher energy collisional dissociation fragmentation with a AGC value of $1e^5$. The isolation of the precursors was performed with a 1.6 m/z window. The survey scans were performed at a resolution of 120,000 (at *m/z* 200), whereas the resolution for HCD spectra was set to 15,000 (at *m/z* 200) with a maximum ion injection time of 35 ms. The fragmentation was performed at the normalized collision energy of 27 eV. The precursor ions with single, unassigned, or six and higher charge states were excluded from the fragmentation.

Analysis of Untargeted Proteomics Data: The DDA data were processed with MaxQuant version 1.6.8.0 (Max-Planck Institute for Biochemistry, Planegg, Germany) using Andromeda search engine (Tyanova et al., 2016a), in which the high-resolution MS/MS spectra were searched against the human liver proteome database (15,656 proteins) curated from UniPort (www.uniprot.org). A decoy database constructed within MaxQuant was employed to control the false discovery rate (FDR). Trypsin was selected as the proteolytic enzyme with a maximum of two missed cleavages. Carbamidomethylation of cysteine was selected as a fixed modification, and N-terminal acetylation and methionine oxidation were selected as variable modifications. Peptides were searched with the mass tolerance of 5 ppm (at MS1 level) and 10 ppm (at MS2 level). Both peptide and protein FDR were set to a maximum value of 1%. Only surrogate

10

(unique) peptides were selected for the protein quantification based on label free quantitation (LFQ). The MaxQuant data were processed using Perseus software (1.6.8.0) (Tyanova et al., 2016b), where the following hits were first removed: contaminants, proteins identified by the reverse sequence, and proteins identified in only one replicate out of three (ambiguous identification). Principal component analysis (PCA) of the shortlisted data was performed to identify the group-dependent clustering of the replicates and to visualize if the liver proteome is different between two groups (UGT2B17 deletion *versus* high expressers). Further orthogonal partial least squares discriminant analysis (OPLS-DA) analysis was performed for the two groups which was utilized to identify proteins significantly different in these groups by S-plot. The differentially expressed proteins obtained from S-plot with P value <0.05 were subjected to pathway analysis using STRING (Szklarczyk et al., 2015). The protein interactome was generated with list of both upregulated and downregulated protein to characterize the protein-protein interactions and associated molecular and biological pathways by the functional protein association network analysis using STRING database (https://string-db.org).

Characterization of alternate testosterone metabolism pathways in UGT2B17 gene deletion subjects

Testosterone metabolism by aldoketoreductases: Cytosolic fraction, isolated from liver tissues of UGT2B17 deletion carriers (2 males and 1 female), were used for the AKR activity. AKR activity assay was performed in a reaction buffer (100 μL) containing 100 mM sodium phosphate buffer (pH 7.4), 1 mM ethylenediaminetetraacetic Acid (EDTA) and 10 μM substrate (testosterone or 5β-DHT). The sample was vortex-mixed and pre-incubated for at 37 °C for 5 min before initiating the reaction by adding NADPH cofactor and performing the time-dependent product formation assay for 0, 5, 10, 15, 30, 45, and 60 min. The samples were mixed and centrifuged at 4 °C at 3200 x g (5 min). The supernatant was collected and diluted 2-fold with

0.1% formic acid and analysis of testosterone,5β-DHT and 3α,5β-THT was conducted using an optimized LC-MS/MS (Xevo TQXS, Waters, Milford, MA) (Supplementary Table S1).

Glucuronidation of reduced testosterone metabolites: Glucuronidation assay of the metabolites formed by AKRs was performed in recombinant human UGT2Bs (10 μg/ml, final protein). The reaction buffer consists of 5 mM $MgCl_2$-100 mM phosphate buffer (pH 7.4), alamethicin (0.1 mg/mL), and BSA (0.02%). The substrates, 5β-DHT and 3α,5β-THT (1 μM) were added to the reaction mixture, which was incubated with alamethicin in ice for 15 min to allow the pore formation. The reaction was performed for 30 min at 37 °C after adding UDPGA (2.5 mM). Ice cold acetonitrile containing internal standard (epitestosterone glucuronide) was used for quenching the reaction followed by centrifugation at 2000 × g, 4°C (5 min). The supernatant was mixed with 0.1% formic acid 1:1 (v/v) to reduce the organic content and analyzed by LC-MS/MS to quantify the substrate depletion and the formation of the corresponding glucuronide metabolite using the parameters provided in Supplementary Table S1.

Effect of UGT2B17 variability on in vitro metabolism of testosterone in human hepatocytes: We first identified four cryopreserved hepatocyte lots (two high and two low UGT2B17 expressing) based on targeted proteomics experiment as described previously (Basit et al., 2018). The selected hepatocytes (n=4) were thawed for at 37 °C for 60-90 seconds and resuspended in 12 mL hepatocyte thawing (HT) media previously warmed to 37 °C. The hepatocytes were centrifuged at room temperature at 100 g for 5 min. The supernatant was discarded without disturbing the cell pellet, and cells were resuspended in 3 mL of hepatocyte incubation (HI) media. Cell count was carried out using Nexcelom Bioscience Cellometer Auto T4 (Lawrence, MA) and the HI media was added to cell suspension to maintain 0.6×10^6 cells per mL. Reaction was initiated with the addition of 150 μL of hepatocyte suspension to 150 μL prewarmed HI media containing testosterone (200 μM) in a 24 well plate. The final 0.3 mL sample contained 0.3 million cells and 100 μM testosterone in each well was incubated for 60

12

min (37 °C) at 100 rpm. The reaction was quenched with 0.6 mL of acetonitrile containing internal standard mix. The incubation mixture was transferred to a 1.7 mL tube, mixed vigorously for 1 minute and centrifuged at 8000 xg (10 min). The supernatant (100 μL) was acidified by 0.1% formic acid (100 μL) and transferred to an LC-MS vial.

Activation of testosterone by bacterial β-glucuronidases

Ex vivo fecal deconjugation of testosterone glucuronide: The glucuronide deconjugation assay was performed using a previously optimized protocol (Ervin et al., 2019). In brief, the reaction mixture contains 30 μL water, 10 μL of 25 nM HEPES buffer (pH 6.5) with 25 mM NaCl, 5 μL fecal samples (0.1 mg/mL protein) was preincubated at 37 °C for 5 min. The substrate (5 μL TG, 1 μM) was added and incubated for 30 min at 37 °C. The purified *Eubacterium eligens (E. eligens)* GUS (10 μg/mL) was used as a potential positive control in this assay as it universally metabolizes multiple glucuronide substrates (Pollet et al., 2017). The reaction was quenched by adding ice cold acetonitrile containing testostosterone-d3, 25 nM (internal standard) and the conjugated and deconjugated testosterone were analyzed using LC-MS/MS using an optimized method (Basit et al., 2018) with some modifications shown in Supplementary Table S1.

Screening of bacterial β-glucuronidases for the deconjugation of testosterone glucuronide: To identify the role of individual GUS capable of TG deconjugation, we performed the assay using 10 different GUS enzymes using optimized final enzyme concentrations and pH provided in Supplementary Table S2. The reaction containing 20 μl assay buffer, 10 μl enzyme (various concentrations provided in Supplementary Table S2), and 20 μl substrate (50 μM, final 20 μM), in 50 μl of total volume was carried out at 37 °C (30 min). The variable final enzyme concentrations were selected based on the relative activities of these enzymes against the standard GUS substrate, p-nitrophenol glucuronide (Pollet et al., 2017). The reaction was quenched with 100 μl of the ice-cold acetonitrile containing testosterone-d3. The samples were vortex-mixed to allow for mechanical lysis and centrifuge at 13,000 x g for 10 min (4 °C). The

supernatant (100 µl) was transferred to LC-MS vial for the analysis by SCIEX 6500 MS (Framingham, MA) coupled with Waters Acquity UPLC (Waters, Milford, MA) (Supplementary Table S3). The testosterone concentration was determined using a standard curve (range, 0.1 to 50 ng/ml).

TG disappearance with time in the presence of GUS enzymes: The in vitro TG disappearance assay by GUS enzymes isolated from *Escherichia coli (E. Coli)* and *E. eligens* was conducted at 37 °C in the total volume of 50 µl. A reaction consisted of 10 µl of incubation buffer (50 mM HEPES, 50 mM NaCl buffer pH 6.5), 10 µl of GUS enzyme (*E. coli* and *E. eligens* diluted to 5 nM, final concentration of 1 nM), and 30 µl of substrate (final concentration, 10 µM) diluted in the incubation buffer. The reactions were quenched at 5, 10, 15, 20, 30, 45, 60, 75, and 90 min after the start of incubation with acetonitrile containing testosterone-d3 as internal standard. The samples were centrifuged and analyzed using protocol described above. TG disappearance rate (0 min versus individual time points) was compared using ANOVA followed by Dunnett's T3 multiple comparisons test, with $*p<0.05$, $**p<0.01$, $***p<0.001$.

In vivo confirmation of AKR pathway

Untargeted metabolomics analysis of plasma samples with oral testosterone dosing in man: Serum samples from healthy men participating in a University of Washington IRB approved study of oral testosterone administration were used (Amory and Bremner, 2005). All subjects provided written consents for the participation. The serum samples were pooled from all time points after a single oral dose of testosterone in oil 800 mg in men (n=7). Predose-testosterone administration samples were used as controls. Testosterone and its metabolic products were extracted using protein precipitation by ice cold methanol containing internal standard mix (deuterated steroids) followed by solid-phase extraction (SPE) using C18 HLB cartridges (Waters, Milford, MA). Briefly, serum samples (200 µL) were transferred to 1.5 mL tubes, and protein precipitation was performed using 5-fold higher volume of the internal standard mix.

14

Samples were vortex-mixed and centrifuged for at 5000 × g for 10 min (4°C). The supernatant was dried under nitrogen evaporator in a glass tube, and the residue was redissolved in 2 mL of 5% methanol containing 0.1% formic acid. The SPE cartridges were activated by 2 mL methanol and conditioned by 2 mL 0.1% formic acid before sample (2 mL) loading. The flow-through was discarded and the samples were washed with 1 mL of 5% methanol. Analytes were eluted with methanol (2 mL) in a glass tube and dried under nitrogen evaporator. The reconstituted sample in 0.1 mL 10% acetonitrile was transferred to an LC-MS vial.

The extracted metabolomic samples were analyzed in data-dependent acquisition (DDA) mode by LC-MS (EASY-nLC 1200 and Q-Exactive HF MS; Thermo Fisher Scientific , Waltham, MA). Sample was loaded onto a C18 trap column (100 µm × 2 cm, 5 µm, Acclaim PepMap) and desalted for 10 min with 0.1% formic acid. The trapped sample was then eluted through a C18 column (Thermo Scientific™ PepMap™; 50 µm × 15 cm, 2 µm). The metabolites were separated with 0.3 µL/min mobile phase using the following gradient condition. 0.0–5.0 min. (10% B), 5.0–45 min (10–40% B), 45–65 min (40–80% B), 65–69.0 min (80% B), and then equilibrated back to 10% B for 10 min. Metabolites were detected in data-dependent acquisition (DDA) mode, where the top ten most intense ions from the MS1 scan were selected for the fragmentation by collision induced dissociation. The survey scans of metabolites were performed in Orbitrap from 100 to 1000 m/z (resolution of 120,000 at 200 m/z) with a 3×10^6 ion count target and the maximum injection time of 100 ms. The MS/MS resolution was set to 15,000 with AGC target of 1×10^5 with the isolation window of 1.6 m/z. The collision energy was 27 eV. The untargeted metabolomics data was analyzed using open XCMS online. The raw data file was uploaded and pairwise analysis was performed to compare the metabolomics difference between two groups.

RESULTS

Association of UGT2B17 gene deletion with the liver proteome in man

15

Global proteomics analysis of post-mitochondrial (S9) fraction of liver tissue from individuals harboring UGT2B17 deletion and high expresser genotypes revealed a direct impact of UGT2B17 on hepatic metabolism pathways. We quantified a total of 1002 proteins in the study with a stringent criterion of a minimum two peptides and at least one signature peptide per protein. Out of these, 949 proteins were common in the deletion and expresser subjects, while 14 and 39 proteins were unique to each group, respectively (Fig. 2A). The PCA and OPLS-DA confirmed the clustering of the samples into two groups (Fig. 2B). Eighty-four proteins were significantly upregulated in UGT2B17 deletion subjects while 89 proteins were significantly downregulated (Fig. 2C and Supplementary Fig. S1). STRING analysis on the upregulated proteins revealed that most of these proteins are associated with oxidoreductase pathways, including AKRs and aldehyde dehydrogenase (*e.g.,* AKR1D1, AKR1C4, AKR1A1, and AKR7A3 were significantly upregulated) (Fig. 2D). These proteins play important roles in steroid and bile acid biosynthesis and metabolism (Penning et al., 2019). We also observed that UGT2B7 was significantly upregulated in the UGT2B17 deletion group.

Confirmation of alternate testosterone metabolism pathways in UGT2B17 deletion subjects

Clinical pharmacokinetic data suggest that testosterone is primarily metabolized to androstenedione, AG, EtioG and TG in adult men (Basit et al., 2018). Interestingly, in the UGT2B17 deletion subjects, AKR1D1, AKR1C4 and UGT2B7 enzymes were upregulated, suggesting a major role of these alternate pathways in testosterone disposition in the setting of UGT2B17 gene deletion. These data suggest metabolic switching in UGT2B17 gene deletion subjects leading to conversion of testosterone to 5β-DHT by AKR1D1, which is subsequently metabolized to, 3α, 5β -THT by AKR1C4 (Chen et al., 2011). Further, 3α,5β-THT is glucuronidated at 3α-position by another UGT isoform, UGT2B7, which is subsequently eliminated by the kidneys. The *in vitro* AKR assay in the liver cytosol confirmed the formation of

16

5β-DHT from testosterone, and 3α,5β-THT from 5β-DHT in a time-dependent manner (Fig. 3 and Supplementary Fig. S2). 5β-DHT is selectively glucuronidated by UGT2B17, whereas glucuronidation of 3α,5β-THT at 3-position and 17-position is mediated by UGT2B7 and UGT2B17, respectively (Fig. 3D-E). Therefore, the major route of THT glucuronidation in UGT2B17 deletion subjects is through 3-glucuronide formation via UGT2B7. Testosterone metabolism in human hepatocytes also confirmed high activity of AKR1D1 and AKR1C4 in the low UGT2B17 expressers. The AKR activities were higher in the hepatocytes with low UGT2B17 activity (Supplementary Fig. S3).

In vivo confirmation of AKR pathway

The qualitative presence of metabolites highlighting the AKR pathway was confirmed in serum samples of men who were administered with 800 mg of oral testosterone. The exogenous testosterone led to formation of AKR-mediated THT glucuronide metabolites that were higher in serum of men exposed to exogenous testosterone than the control serum, while phase I metabolites (DHT and THT) were below the detection limit (Fig. 4).

Activation of testosterone glucuronide to testosterone by microbial GUS enzymes

TG to testosterone conversion in human fecal samples ex vivo indicates the clinical significance of GUS enzymes in testosterone activation in the GI tract. While all ex vivo samples processed TG to testosterone, the sample from male 1 produced more testosterone than did the sample from male 2, with the sample from the female donor being intermediate between the two male samples (Fig. 5A). To identify gut microbial β-glucuronidase (GUS) enzymes capable of deconjugating TG to testosterone, we examined ten distinct GUS enzymes that were previously cloned, expressed, and purified (Ervin et al., 2019). The enzymes employed represented the major gut microbial phyla, as well as the functional clades established for this diverse group of bacterial enzymes (Pollet et al., 2017). We found that all the GUS enzymes studied were able

to deconjugate TG back to reactivated testosterone (Fig. 5B), although varying degrees of conversion were observed. These differential abilities to reactivate testosterone from TG were also observed using *E. coli* and *E. eligens* GUS enzymes and time course studies conducted over 90 min, which revealed that *E. coli* GUS exhibited greater TG processing relative to *E. eligens* GUS (Figs 5C and 5D). Taken together, these results show that gut microbial GUS enzymes can reactivate TG to testosterone with varying efficiencies represented in both purified proteins *in vitro* and fecal extracts *ex vivo*.

DISCUSSION

To understand the association of UGT2B17 deletion with the liver proteome and metabolome we performed untargeted proteomics study comparing liver S9 proteome in individuals harboring UGT2B17 deletion and high expression genotypes followed by a series of in vitro experiments to validate the findings. The proteomics data revealed that the upregulated proteins were associated with the aldoketoreducase (AKR) family. These enzymes catalyze NADPH-dependent reduction of the steroidal ring at C3, C5, C17 and C20 positions (Rizner and Penning, 2014). We identified that AKR1D1 and AKR1C4 could play critical roles in testosterone metabolism in UGT2B17 non-expressers, which needs further in vivo investigation if the metabolic switching in UGT2B17 gene deletion subjects changes the rate of testosterone elimination or half-life of testosterone. AKR1D1 is selectively expressed in the liver with minor expression in the fallopian tube and breast, whereas AKR1C4 is ubiquitously expressed across various tissues with highest expression in the liver (Barski et al., 2008). AKR1D1 is the only human enzyme that stereospecifically reduces Δ^4 double bond of steroidal ring to 5β-dihydro steroid and generates the 5β-reduced dihydrosteroidal metabolites for C19, C21 and C27 steroids including androgens, glucocorticoids, and bile acids (Nikolaou et al., 2019). Further, AKR1C4 is the major enzyme responsible for the reduction of 3-keto steroids to 3α-hydroxy steroids. These two enzymes work in tandem to metabolize testosterone to 5β-DHT and

18

subsequently to 3α,5β-THT in individuals with UGT2B17 gene deletion. The in vitro activity data at lower testosterone concentration (Supplementary Fig. S2) suggest that the intermediate 5β-DHT is immediately transformed to 3α,5β-THT by AKR1C4, and is unlikely to be accumulated in the liver. 3α,5β-THT is then metabolized by UGT2B7 that is also upregulated in UGT2B17 deletion subjects and is likely excreted as the glucuronide in urine. We have confirmed this metabolic switching through a series of in vitro experiments (Fig. 4). However, it requires in vivo investigations if the perturbation in AKR1D1 activity in UGT2B17 deletion subjects will lead to a higher circulating testosterone. AKRs (AKR1C1-1C4) play important roles in pathophysiology of prostate, breast, and endometrial cancer (Penning and Byrns, 2009). Similarly, UGT2B17 gene deletion is associated with prostate cancer risk (Kpoghomou et al., 2013; Gauthier-Landry et al., 2015), lower body mass index (BMI), higher fat mass (Chew et al., 2011; Zhu et al., 2015), increased bone mineral density, and decreased osteoporotic fractures (Yang et al., 2008; Che et al., 2015). Our findings indicate the mechanistic interplay of AKR and UGT2B17, which needs further investigation to understand the molecular mechanisms. AKR1D1 dysregulation and mutation are linked to bile acid deficiency (Drury et al., 2010). AKR1D1 knockdown in HepG2, Huh7 cells, and human hepatocytes lead to an increased de novo lipogenesis and accumulation of triacylglycerol indication of obese phenotype (Nikolaou et al., 2019). The upregulation of AKR1D1 is not well studied leading to a critical knowledge gap with respect to the pathophysiological role of AKR1D1.

This study also examined the role of gut microbial enzymes in deconjugating TG back to reactivated testosterone. Although the importance of gut microbial GUS enzymes in processing steroid hormone glucuronides is not novel (Ervin et al., 2019), this is the first analysis of TG hydrolysis by these bacterial proteins. Integration of TG fecal processing rates with proteomics-based GUS enzyme quantification would be a powerful addition to physiologically based pharmacokinetic (PBPK) modeling. These mechanistic findings may help understanding the

mechanisms of testosterone associated pathophysiology such as obesity, prostate cancer, lung cancer, endometrial cancer, and doping. Our deconjugation data are supported by recent studies indicating high concentration of free testosterone in colon in both men and mice (Collden et al., 2019).

In summary, this exploratory study highlights the potential importance of AKR pathway in testosterone metabolism in UGT2B17 deletion or compromised subjects. Our data suggest that AKR1D1, which is expressed selectively in the liver, likely plays an important role in detoxifying excess testosterone in the absence of UGT2B17 activity. Therefore, modulation of AKR1D1 activity in UGT2B17-compromised individuals may cause testosterone associated side effects. 5β-DHT formed by AKR1D1 activity is rapidly metabolized by AKR1C4 to 3α,5β-THT and subsequently eliminated as glucuronide products. The newer insights on testosterone metabolism are potentially important for explaining disposition of exogenously administered testosterone and clinical conditions associated with UGT2B17 deletion, e.g., prostate cancer (Gallagher et al., 2007), endometrial cancer (Hirata et al., 2010), chronic lymphocytic leukemia (Gruber et al., 2013), and obesity (Zhu et al., 2015). Further, 5β-DHT, 3α, 5β-THT and their subsequent metabolites can be added in doping test panel to avoid false negative and positive outcomes due to UGT2B17 variability. Similarly, the mechanistic insights on the role of microbiome in testosterone activation in gut can be leveraged in controlling variability in testosterone exposure after exogenous administered and explaining microbiome associated pathophysiology.

Supplementary information

Supplementary data are available.

Experimental workflow, protein interactome analysis by STRING from downregulated proteins in UGT2B17 deletion, Correlation between TG and THT formation from testosterone incubation in human hepatocyte and LC-MS/MS parameters for the quantification of testosterone and its metabolites.

ACKNOWLEDGEMENTS

AUTHOR CONTRIBUTIONS

A.B., J.K.A., M.R.R and B.P. wrote the manuscript.

A.B., and B.P. designed the research experiments.

A.B., V.S. M., CYL and P.B.J. performed the research experiments.

A.B. and B.P. analyzed the data.

S.H. contributed to reagent.

REFERENCES

Amory JK and Bremner WJ (2005) Oral testosterone in oil plus dutasteride in men: a pharmacokinetic study. *J Clin Endocrinol Metab* **90**:2610-2617.

Balhara A, Basit A, Argikar UA, Dumouchel JL, Singh S and Prasad B (2021) Comparative Proteomics Analysis of the Postmitochondrial Supernatant Fraction of Human Lens-Free Whole Eye and Liver. *Drug Metab Dispos* **49**:592-600.

Barski OA, Tipparaju SM and Bhatnagar A (2008) The aldo-keto reductase superfamily and its role in drug metabolism and detoxification. *Drug Metab Rev* **40**:553-624.

Basit A, Amory JK and Prasad B (2018) Effect of Dose and 5alpha-Reductase Inhibition on the Circulating Testosterone Metabolite Profile of Men Administered Oral Testosterone. *Clin Transl Sci* **11**:513-522.

Bhasin S, Cunningham GR, Hayes FJ, Matsumoto AM, Snyder PJ, Swerdloff RS and Montori VM (2006) Testosterone therapy in adult men with androgen deficiency syndromes: an endocrine society clinical practice guideline. *J Clin Endocrinol Metab* **91**:1995-2010.

Bhasin S, Cunningham GR, Hayes FJ, Matsumoto AM, Snyder PJ, Swerdloff RS, Montori VM and Task Force ES (2010) Testosterone therapy in men with androgen deficiency syndromes: an Endocrine Society clinical practice guideline. *J Clin Endocrinol Metab* **95**:2536-2559.

Bhasin S and Matsumoto AM (2010) Patient information page from The Hormone Foundation. Patient guide to testosterone therapy in adult men with androgen deficiency syndromes. *J Clin Endocrinol Metab* **95**:2p following 3085.

Bhatt DK and Prasad B (2018) Critical Issues and Optimized Practices in Quantification of Protein Abundance Level to Determine Interindividual Variability in DMET Proteins by LC-MS/MS Proteomics. *Clin Pharmacol Ther* **103**:619-630.

Che X, Yu D, Wu Z, Zhang J, Chen Y, Han Y, Wang C and Qi J (2015) Association of Genetic Polymorphisms in UDP-Glucuronosyltransferases 2B17 with the Risk of Pancreatic Cancer in Chinese Han Population. *Clin Lab* **61**:1905-1910.

Chen M, Drury JE and Penning TM (2011) Substrate specificity and inhibitor analyses of human steroid 5beta-reductase (AKR1D1). *Steroids* **76**:484-490.

Chew S, Mullin BH, Lewis JR, Spector TD, Prince RL and Wilson SG (2011) Homozygous deletion of the UGT2B17 gene is not associated with osteoporosis risk in elderly Caucasian women. *Osteoporos Int* **22**:1981-1986.

Collden H, Landin A, Wallenius V, Elebring E, Fandriks L, Nilsson ME, Ryberg H, Poutanen M, Sjogren K, Vandenput L and Ohlsson C (2019) The gut microbiota is a major regulator of androgen metabolism in intestinal contents. *Am J Physiol Endocrinol Metab* **317**:E1182-E1192.

Drury JE, Mindnich R and Penning TM (2010) Characterization of disease-related 5beta-reductase (AKR1D1) mutations reveals their potential to cause bile acid deficiency. *J Biol Chem* **285**:24529-24537.

Ervin SM, Li H, Lim L, Roberts LR, Liang X, Mani S and Redinbo MR (2019) Gut microbial beta-glucuronidases reactivate estrogens as components of the estrobolome that reactivate estrogens. *J Biol Chem* **294**:18586-18599.

FDA U (2015) Testosterone Information, in.

Gallagher CJ, Kadlubar FF, Muscat JE, Ambrosone CB, Lang NP and Lazarus P (2007) The UGT2B17 gene deletion polymorphism and risk of prostate cancer. A case-control study in Caucasians. *Cancer Detect Prev* **31**:310-315.

Gauthier-Landry L, Belanger A and Barbier O (2015) Multiple roles for UDP-glucuronosyltransferase (UGT)2B15 and UGT2B17 enzymes in androgen metabolism and prostate cancer evolution. *J Steroid Biochem Mol Biol* **145**:187-192.

Gruber M, Bellemare J, Hoermann G, Gleiss A, Porpaczy E, Bilban M, Le T, Zehetmayer S, Mannhalter C, Gaiger A, Shehata M, Fleiss K, Skrabs C, Levesque E, Vanura K, Guillemette C and Jaeger U (2013) Overexpression of uridine diphospho glucuronosyltransferase 2B17 in high-risk chronic lymphocytic leukemia. *Blood* **121**:1175-1183.

Hirata H, Hinoda Y, Zaman MS, Chen Y, Ueno K, Majid S, Tripsas C, Rubin M, Chen LM and Dahiya R (2010) Function of UDP-glucuronosyltransferase 2B17 (UGT2B17) is involved in endometrial cancer. *Carcinogenesis* **31**:1620-1626.

Jakobsson J, Ekstrom L, Inotsume N, Garle M, Lorentzon M, Ohlsson C, Roh HK, Carlstrom K and Rane A (2006) Large differences in testosterone excretion in Korean and Swedish men are strongly associated with a UDP-glucuronosyl transferase 2B17 polymorphism. *J Clin Endocrinol Metab* **91**:687-693.

Juul A, Sorensen K, Aksglaede L, Garn I, Rajpert-De Meyts E, Hullstein I, Hemmersbach P and Ottesen AM (2009) A common deletion in the uridine diphosphate glucuronyltransferase (UGT) 2B17 gene is a strong determinant of androgen excretion in healthy pubertal boys. *J Clin Endocrinol Metab* **94**:1005-1011.

Kpoghomou MA, Soatiana JE, Kalembo FW, Bishwajit G and Sheng W (2013) UGT2B17 Polymorphism and Risk of Prostate Cancer: A Meta-Analysis. *ISRN Oncol* **2013**:465916.

Li CY, Basit A, Gupta A, Gaborik Z, Kis E and Prasad B (2019) Major glucuronide metabolites of testosterone are primarily transported by MRP2 and MRP3 in human liver, intestine and kidney. *J Steroid Biochem Mol Biol* **191**:105350.

Li CY, Gupta A, Gaborik Z, Kis E and Prasad B (2020) Organic Anion Transporting Polypeptide-Mediated Hepatic Uptake of Glucuronide Metabolites of Androgens. *Mol Pharmacol* **98**:234-242.

Mazer N, Bell D, Wu J, Fischer J, Cosgrove M, Eilers B and Bs RN (2005) Comparison of the steady-state pharmacokinetics, metabolism, and variability of a transdermal testosterone patch versus a transdermal testosterone gel in hypogonadal men. *J Sex Med* **2**:213-226.

Nikolaou N, Gathercole LL, Marchand L, Althari S, Dempster NJ, Green CJ, van de Bunt M, McNeil C, Arvaniti A, Hughes BA, Sgromo B, Gillies RS, Marschall HU, Penning TM, Ryan J, Arlt W, Hodson L and Tomlinson JW (2019) AKR1D1 is a novel regulator of metabolic phenotype in human hepatocytes and is dysregulated in non-alcoholic fatty liver disease. *Metabolism* **99**:67-80.

Penning TM and Byrns MC (2009) Steroid hormone transforming aldo-keto reductases and cancer. *Ann N Y Acad Sci* **1155**:33-42.

Penning TM, Wangtrakuldee P and Auchus RJ (2019) Structural and Functional Biology of Aldo-Keto Reductase Steroid-Transforming Enzymes. *Endocr Rev* **40**:447-475.

Pollet RM, D'Agostino EH, Walton WG, Xu Y, Little MS, Biernat KA, Pellock SJ, Patterson LM, Creekmore BC, Isenberg HN, Bahethi RR, Bhatt AP, Liu J, Gharaibeh RZ and Redinbo MR (2017) An Atlas of beta-Glucuronidases in the Human Intestinal Microbiome. *Structure* **25**:967-977 e965.

Rane A and Ekstrom L (2012) Androgens and doping tests: genetic variation and pit-falls. *Br J Clin Pharmacol* **74**:3-15.

Rizner TL and Penning TM (2014) Role of aldo-keto reductase family 1 (AKR1) enzymes in human steroid metabolism. *Steroids* **79**:49-63.

Schlich C and Romanelli F (2016) Issues Surrounding Testosterone Replacement Therapy. *Hosp Pharm* **51**:712-720.

Schulze JJ, Lundmark J, Garle M, Ekstrom L, Sottas PE and Rane A (2009) Substantial advantage of a combined Bayesian and genotyping approach in testosterone doping tests. *Steroids* **74**:365-368.

Schulze JJ, Lundmark J, Garle M, Skilving I, Ekstrom L and Rane A (2008) Doping test results dependent on genotype of uridine diphospho-glucuronosyl transferase 2B17, the major enzyme for testosterone glucuronidation. *J Clin Endocrinol Metab* **93**:2500-2506.

Spanos C, Bretherton I, Zajac JD and Cheung AS (2020) Effects of gender-affirming hormone therapy on insulin resistance and body composition in transgender individuals: A systematic review. *World J Diabetes* **11**:66-77.

Strahm E, Mullen JE, Garevik N, Ericsson M, Schulze JJ, Rane A and Ekstrom L (2015) Dose-dependent testosterone sensitivity of the steroidal passport and GC-C-IRMS analysis in relation to the UGT2B17 deletion polymorphism. *Drug Test Anal* **7**:1063-1070.

Swerdloff RS, Pak Y, Wang C, Liu PY, Bhasin S, Gill TM, Matsumoto AM, Pahor M, Surampudi P and Snyder PJ (2015) Serum Testosterone (T) Level Variability in T Gel-Treated Older Hypogonadal Men: Treatment Monitoring Implications. *J Clin Endocrinol Metab* **100**:3280-3287.

Szklarczyk D, Franceschini A, Wyder S, Forslund K, Heller D, Huerta-Cepas J, Simonovic M, Roth A, Santos A, Tsafou KP, Kuhn M, Bork P, Jensen LJ and von Mering C (2015) STRING v10: protein-protein interaction networks, integrated over the tree of life. *Nucleic Acids Res* **43**:D447-452.

Tyanova S, Temu T and Cox J (2016a) The MaxQuant computational platform for mass spectrometry-based shotgun proteomics. *Nat Protoc* **11**:2301-2319.

Tyanova S, Temu T, Sinitcyn P, Carlson A, Hein MY, Geiger T, Mann M and Cox J (2016b) The Perseus computational platform for comprehensive analysis of (prote)omics data. *Nat Methods* **13**:731-740.

Wilson DM, Kiang TKL and Ensom MHH (2018) Pharmacokinetics, safety, and patient acceptability of subcutaneous versus intramuscular testosterone injection for gender-affirming therapy: A pilot study. *Am J Health Syst Pharm* **75**:351-358.

Xue Y, Sun D, Daly A, Yang F, Zhou X, Zhao M, Huang N, Zerjal T, Lee C, Carter NP, Hurles ME and Tyler-Smith C (2008) Adaptive evolution of UGT2B17 copy-number variation. *Am J Hum Genet* **83**:337-346.

Yang TL, Chen XD, Guo Y, Lei SF, Wang JT, Zhou Q, Pan F, Chen Y, Zhang ZX, Dong SS, Xu XH, Yan H, Liu X, Qiu C, Zhu XZ, Chen T, Li M, Zhang H, Zhang L, Drees BM, Hamilton JJ, Papasian CJ, Recker RR, Song XP, Cheng J and Deng HW (2008) Genome-wide copy-number-variation study identified a susceptibility gene, UGT2B17, for osteoporosis. *Am J Hum Genet* **83**:663-674.

Zhang H, Basit A, Busch D, Yabut K, Bhatt DK, Drozdzik M, Ostrowski M, Li A, Collins C, Oswald S and Prasad B (2018) Quantitative characterization of UDP-glucuronosyltransferase 2B17 in human liver and intestine and its role in testosterone first-pass metabolism. *Biochem Pharmacol* **156**:32-42.

Zhu AZ, Cox LS, Ahluwalia JS, Renner CC, Hatsukami DK, Benowitz NL and Tyndale RF (2015) Genetic and phenotypic variation in UGT2B17, a testosterone-metabolizing enzyme, is associated with BMI in males. *Pharmacogenet Genomics* **25**:263-269.

FOOTNOTE

Conflicts of interest: M.R.R. is cofounder of Symberix, Inc, and is the recipient of research funding from Lilly and Merck. BP is the cofounder of Precision Quantomics Inc and recipient of research funding from Bristol Myers Squibb, Genentech, Gilead, Merck, Takeda, and Generation Bio.

LEGENDS FOR FIGURES

Fig. 1: Testosterone metabolism scheme in the gene deletion and the high expressers of UGT2B17. The lack of testosterone glucuronidation is compensated by the conversion of testosterone to 5β-dihydrotestosterone mediated by AKR1D1 in the UGT2B17 gene deletion subjects.

Fig. 2: Untargeted proteomics data of the post-mitochondrial (S9) fractions isolated from the liver tissue of the UGT2B17 deletion subjects (Del) versus high expressers (HighExp). The Venn diagram represents the number of proteins identified in both the groups and the biological processes and molecular functions associated with significantly upregulated proteins (A). OPLS-DA analysis on the liver proteome shows the clustering of individual samples between the deletion and the high expresser groups (B). The S-plot from OPLS-DA model highlights the differentially expressed proteins in both the groups (C). The protein interactome analysis by STRING analysis of the upregulated proteins in UGT2B17 deletion (D). Significantly upregulated proteins in UGT2B17 gene deletion individuals are associated with aldoketoreductases (AKR1D1, AKR1C4, AKR1A1, AKR7A3, CBR4 and DHCR7, indicated by blue arrows), aldehyde dehydrogenase pathways (ALDH1A1, ALDH5A1, ALDH9A1, ADH1C and ADH6, indicated by black arrows), and UGT2B7 (indicated by green arrow). The protein interactome of the downregulated proteins is presented in Supplementary Fig. S1.

Fig. 3: In vitro testosterone metabolism by aldoketoreductases in liver cytosol samples from the UGT2B17 deletion subjects (A-C) and in the recombinant UGTs (D-F). Testosterone to 5β-dihydrotestosterone (5β-DHT) and 5β-tetrahydrotestosterone (5 β-THT) conversion with time by AKR1D1 and AKR1C4 in the human liver cytosol obtained from the UGT2B17 deletion subjects (A-C). Blk-1 and Blk-2 are the NADPH blank and enzyme blank, respectively. In vitro glucuronidation of 5β-dihydrotestosterone (5β-DHT) and 5β-tetrahydrotestosterone (5β-THT) using recombinant human UGT2B enzymes (D-F). Structures

28

of testosterone, 5β-DHT, 3α,5β-THT, 5β-DHT-glucuronide, 3α,5β-THT-3-glucuronide, and 3α,5β-THT-17-glucuronide are shown in panel A, B, C, D, E and F, respectively.

Fig. 4: Metabolic cloud plot representing differentially elevated metabolites in serum after oral testosterone dosing in men. The cloud plot represents 16 elevated features in human serum sample after oral 800 mg testosterone dose (T800) as compared to the pre-dose (T0) sample (Supplementary Table S4) with p-value<0.01, fold change >35, and m/z range 200-600. Visualization represents p value by color intensity (more intense means lower p-value) and the fold-change by the radius of circle. The whisker-box plots show the elevated levels (MS peak intensity) of TG (M+H, m/z 465.2482) and THTG (M+NH4, m/z 486.3060) after oral 800 mg testosterone administration (T800) as compared to the pre-dose sample (T0).

Fig. 5: In vitro bacterial β-glucuronidase (GUS) activity towards testosterone glucuronide deconjugation. GUS activity towards testosterone glucuronide in fecal samples at 1 μM TG (A). Deconjugation of TG to testosterone by GUS enzymes from various gut bacterial species at 20 μM TG concentration (B). TG disappearance with time in the presence of GUS enzymes from *Escherichia coli* (C) and *Eubacterium eligens* (D) at 10 μM TG concentration. The experiments were performed in triplicates, where % coefficient of variation (%CV) was within 30% as indicated in Figs 5C and 5D. TG disappearance rate (0 min versus individual time points; Fig. 5C and 5D) was compared using ANOVA followed by Dunnett's T3 multiple comparisons test, with *p<0.05, **p<0.01, ***p<0.001.
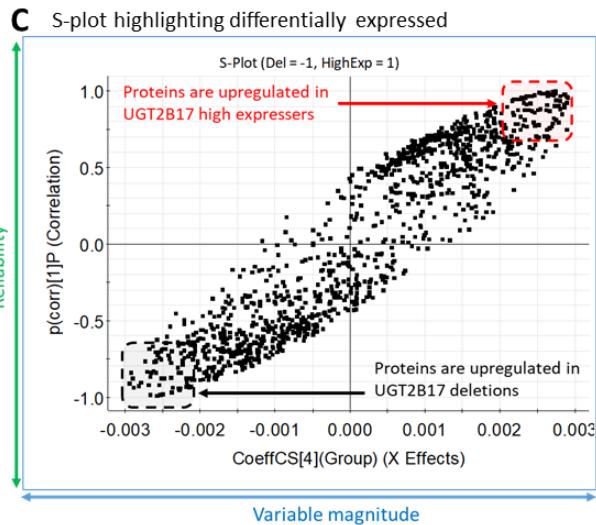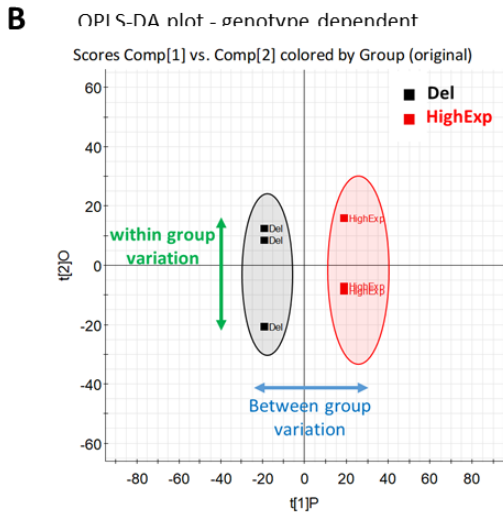
Fig. 1

Fig. 2

Fig. 3

m/z : 465.248
retention time: 38.68 min
p-val : 0.006307
fold change : 849.223 (UP)
max intensity : 36211784
30 matches found.
First three hits :
0 ppm [M+H] Testosterone glu
0 ppm [M+H] Dehydroepiandros
0 ppm [M+H] Dehydroisoandros

m/z : 486.306
retention time: 44.59 min
p-val : 0.008009
fold change : 136.239 (UP)
max intensity : 7664206
30 matches found.
First three hits :
0 ppm [M+NH4] 18-acetoxy-PGF2&
0 ppm [M+NH4] 3α-androst
0 ppm [M+NH4] 3,17-Androstaned

m/z : 431.243
retention time: 47.22 min
p-val : 0.00094
fold change : 584.071 (UP)
max intensity : 44273608
30 matches found.
First three hits :
0 ppm [M+H] Budesonide
0 ppm [M+H] 21-Hydroxypregn-
0 ppm [M+H] Antibiotic CI 15

m/z : 484.29
retention time: 47.31 min
p-val : 0.003212
fold change : 105.420 (UP)
max intensity : 18659946
30 matches found.
First three hits :
0 ppm [M+NH4] 3α-hydroxy
0 ppm [M+NH4] Androsterone glu
0 ppm [M+NH4] Etiocholan-3&alp

e vs *m/z* of 33

in the plot area to z

● **Toggle Upregulated** ○ Toggle Downregulated

TG **THTG**

Feature 465.2/2321   Feature 486.3/2675

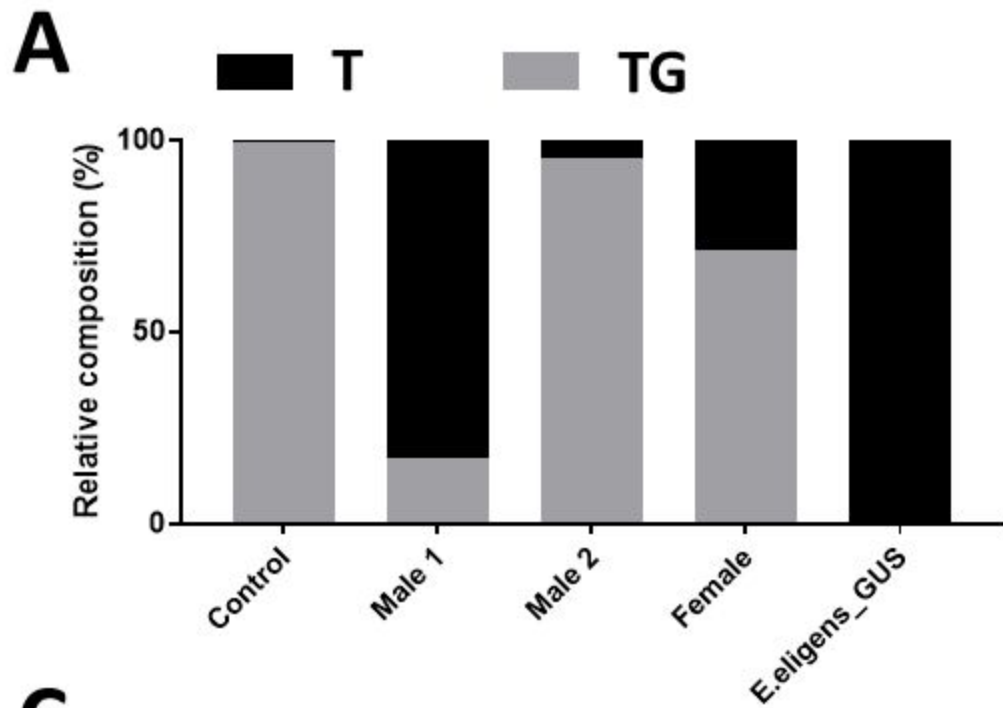*p = 0.006*   *p = 0.008*

Fig. 4

Fig 5

Supplementary Information

Relevance of Human Aldoketoreductases and Microbial β-Glucuronidases in Testosterone Disposition

Abdul Basit[1], John K. Amory[2], Vijay Saradhi Mettu[1], Cindy Yanfei Li[3], Scott Heyward[4], Parth B. Jariwala[5], Matthew R. Redinbo[5] and Bhagwat Prasad[1]

[1]Department of Pharmaceutical Sciences, Washington State University, Spokane, WA

[2]Department of Medicine, University of Washington, Seattle, WA

[3]Department of Pharmaceutics, University of Washington, Seattle, WA

[4]BioIVT Inc., Baltimore, MD

[5]Departments of Chemistry, Biochemistry and Microbiology, and the Integrated Program for Biological and Genome Sciences, University of North Carolina at Chapel Hill, Chapel Hill, NC, USA.

Running title: AKRs and GUSs in Testosterone Disposition

Corresponding author: Bhagwat Prasad, Ph.D., Department of Pharmaceutical Sciences, Washington State University, Spokane, WA 99202, USA. Phone: +1-509-358-7739. Fax: +1 509-368-6561. Email: bhagwat.prasad@wsu.edu
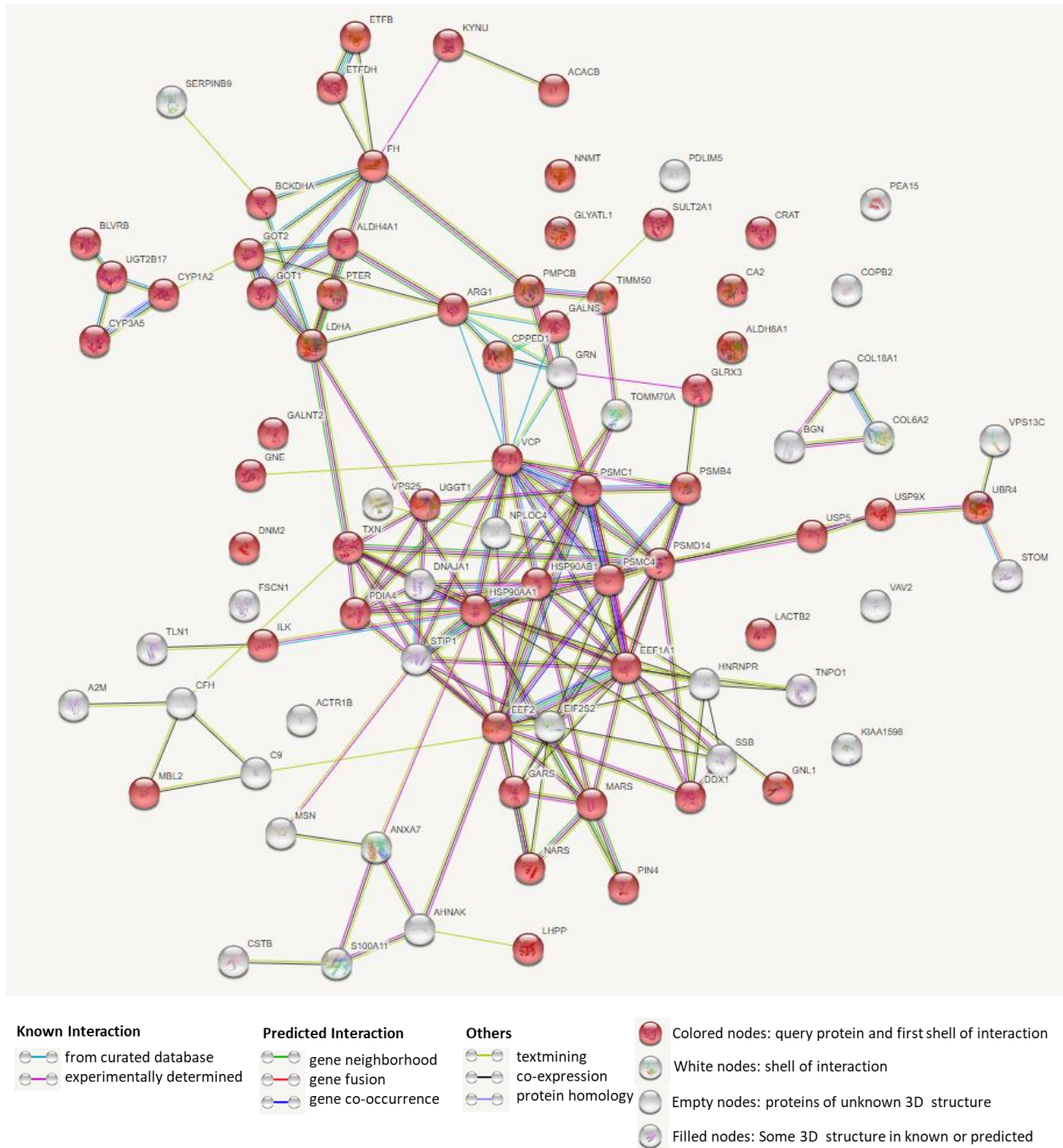
Fig. S1: Protein interactome analysis by STRING from downregulated proteins in UGT2B17 deletion. Significantly downregulated proteins include UGT2B17, CYP3A5, CYP1A2, and SULT2A1
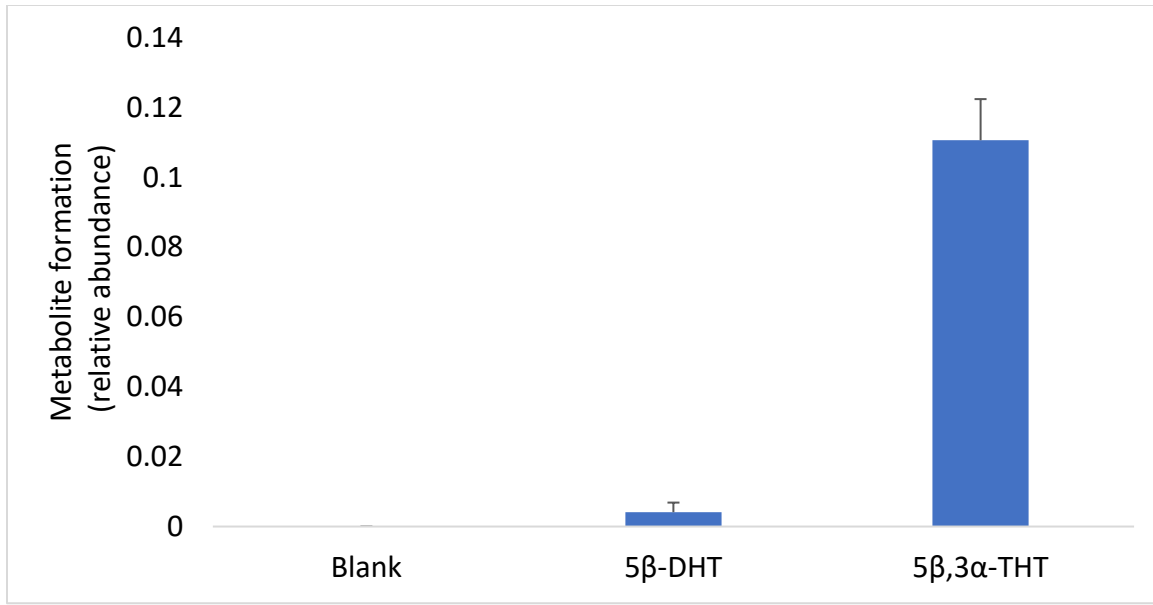
Fig. S2: In vitro formation of testosterone metabolites by AKR pathway when incubated at 1 µM for 30 min with human liver cytosol from UGT2B17 gene deletion subjects.
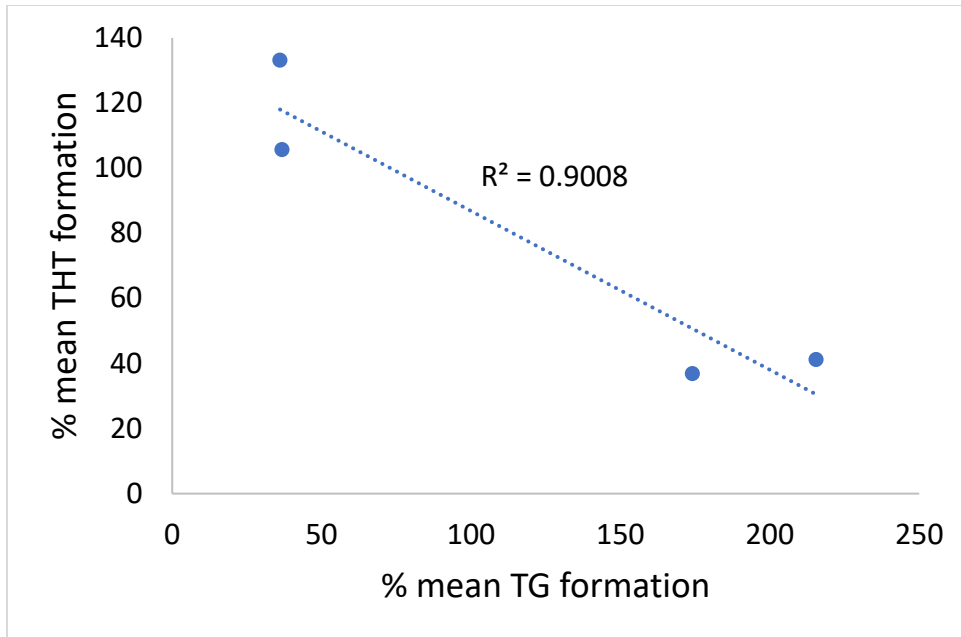
Fig. S3: Negative correlation between TG and THT formation from testosterone incubation in human hepatocytes with high and low UGT2B17 expression.

Table S1: MRM transitions used for quantification of various primary and secondary metabolites of testosterone					
Metabolite	Adduct	Precursor ion (m/z)	Daughter Ion (m/z)	CV (V)	CE (eV)
5β-DHT	[M+H]$^+$	291.1	147.1	30	20
	[M+H]$^+$	291.1	159	30	20
	[M+H]$^+$	291.1	255	30	20
5β, 3α-THT	[M+H-H$_2$O]$^+$	275.1	161	30	20
	[M+H-H$_2$O]$^+$	275.1	174.8	30	15
	[M+H-H$_2$O]$^+$	275.1	257	30	15
5β-DHT-Gluc	[M+H]$^+$	467.1	147.1	30	23
	[M+H]$^+$	467.1	159	30	23
	[M+H]$^+$	467.1	255	30	27
	[M+H]$^+$	467.1	273.1	30	27
5β, 3α-THT-Gluc	[M+H-H$_2$O]$^+$	451.1	161	30	25
	[M+H-H$_2$O]$^+$	451.1	174.8	30	20
	[M+H-H$_2$O]$^+$	451.1	257	30	20
	[M+H-H$_2$O]$^+$	451.1	275.1	30	20
AG-d4	[M+H-H$_2$O]$^+$	453.2	259.2	35	30
	[M+H-H$_2$O]$^+$	453.2	277.4	35	22
	[M+NH$_4$]$^+$	488.3	259.3	35	30
T	[M+H]$^+$	289.1	109.1	35	30
	[M+H]$^+$	289.1	97.1	35	30
T-d3	[M+H]$^+$	292.2	97.1	35	30
	[M+H]$^+$	292.2	109.1	35	30
epiTG	[M+H]$^+$	465.2	289.2	35	30
	[M+H]$^+$	465.2	97.1	35	40
	[M+H]$^+$	465.2	109.1	35	40
TG	[M+H]$^+$	465.2	289.2	35	30
	[M+H]$^+$	465.2	97.1	35	40
	[M+H]$^+$	465.2	109.1	35	40
TG-d3	[M+H]$^+$	468.2	292.2	35	30
	[M+H]$^+$	468.2	97.1	35	40
	[M+H]$^+$	468.2	109.1	35	40

Table S2: Optimized enzyme concentration and pH used for TG deconjugation screening assay using the listed bacterial β-glucuronidases

Bacterial species	Final enzyme concentration (nM)	Optimized pH
Escherichia coli	5	6.5
Eubacterium eligens	5	6.5
Lactobacillus rhamnosus	30	6.5
Bacteroides uniformis	30	6
Roseburia hominis	5	6
Bacteroides fragilis	25	5
Bacteroides ovatus	30	5
Akkermansia muciniphila	20	6.5
Bacteroides coprocola	50	4
Bacteroides nordi	50	5

Table S3: MRM transitions for testosterone and testosterone glucuronide using AB SCIEX 6500					
Metabolite	Adduct	Precursor ion (m/z)	Daughter Ion (m/z)	DP (V)	CE (eV)
T	[M+H]⁺	289.1	109.1	80	30
	[M+H]⁺	289.1	97.1	80	30
TG	[M+H]⁺	465.2	289.2	70	25
	[M+H]⁺	465.2	271.2	70	30
	[M+H]⁺	465.2	109.1	70	35
TG-d3	[M+H]⁺	468.2	292.2	70	25
	[M+H]⁺	468.2	274.2	70	30
	[M+H]⁺	468.2	256.2	70	35
T-d3	[M+H]⁺	292.2	97.1	80	30
	[M+H]⁺	292.2	109.1	80	30

Table S4: Differentially elevated metabolites in serum after oral testosterone dosing in men							
Metabolite ID	Fold-change	P value	Exact mass (m/z)	Predose		Testosterone treated	
				mean1	sd1	mean2	sd2
M486T45	135.8	9.45E-06	486.3061	564555	277163	76673454	14724405
M274T47_2	35.9	1.57E-05	274.2245	2215813	1009919	79627571	16457424
M451T54_1	108.1	7.99E-04	451.3248	448115	624399	48440130	20437127
M403T68_1	376.9	5.21E-07	403.2326	160100	117231	60347036	7121192
M449T47	103.2	7.36E-04	449.2533	695862	805690	71816597	29813267
M520T61_1	56.3	1.50E-03	519.8652	761412	544347	42854221	20225532
M432T47_1	137.3	9.99E-04	432.2461	678100	1070656	93102785	41053663
M234T38	63.2	8.76E-05	234.1699	2008252	369723	126976655	35564331
M484T47_1	105.7	3.08E-08	484.2904	2097666	4619778	221652247	19651543
M238T44_2	70.4	8.51E-07	238.1801	3508011	2393181	246926861	31785644
M376T52_2	103.6	8.55E-04	376.2594	2626951	2706553	272237792	116264603
M302T45_3	51.5	1.19E-03	302.1961	4193737	2531590	216117969	97276040
M450T54_2	42.1	8.69E-04	450.3213	4052959	4876921	170821561	72395557
M274T37_3	189.8	2.23E-06	274.2011	1772298	2057781	336402349	50803785
M465T39_2	846.6	5.71E-05	465.2482	429006	829933	363186969	95756105
M431T47	582.7	9.41E-04	431.2427	592296	293753	345146904	151224744